Electrochemistry of Oxygenation Catalysts. 3.[1] Thermodynamic Characterization of Electron Transfer and Solvent Exchange Reactions of Co(salen)/[Co(salen)]$^+$ in DMF, Pyridine, and Their Mixtures

Emerich Eichhorn, Anton Rieker, Bernd Speiser,*,† and Hartmut Stahl

Institut für Organische Chemie, Auf der Morgenstelle 18, D-72076 Tübingen, Germany

Received March 20, 1997[⊗]

Redox and ligand exchange reactions of the oxygenation catalyst (*N*,*N*′-bis(salicylidene)ethylenediaminato)cobalt(II), Co(salen), and its one-electron oxidation product, Co(salen)$^+$, are investigated in DMF, pyridine, and mixtures of these solvents. Electron transfers and solvent exchange reactions involving three neutral Co(II) and three cationic Co(III) complexes with different axially bound solvent molecules (two DMF, one DMF and one pyridine, or two pyridine molecules) form a three-rung ladder scheme. All formal potentials E^0 and equilibrium constants K in this scheme are determined from electrochemical or spectrophotometric experiments or the construction of thermodynamic cycles. The latter are also used to prove consistency of the results. Values for the E^0 and K are discussed in terms of the Co coordination geometry, solvent effects on the potentials, the thermodynamics of cross reactions, and the distribution of Co(II) and Co(III) species as a function of the solvent composition. Some peculiarities found in the oxygenation of flavonols and indoles are explained.

Introduction

(*N*,*N*′-bis(salicylidene)ethylenediaminato)cobalt(II), Co(salen), **1**,[2,3] is classified as an oxygen carrier[4] and has been

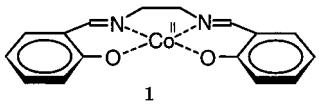

1

used as a catalyst for the preparative oxygenation of phenols,[5−7] indoles,[8,9] flavonols,[10] amines,[11,12] anilines,[13,14] and other substrates[5,15] with both dioxygen or hydroperoxides as the oxygen source. Some authors compare these oxygen transfer reactions to oxygenation by enzymes of mono-, dioxygenase, or peroxidase type, and in some cases, indeed biomimetic activity of the model complex was found.[5,6,10,16,17]

For example, 3-hydroxyflavones readily react with **1**/O_2 in dimethylformamide (DMF) or dimethyl sulfoxide in a quercetinase model reaction,[5] while this reaction is slow in CH_3OH and not observed in dichloromethane (DCM) at all. On the other hand, indoles form *ortho*-(formylamino)acetophenones (formylkynurenines) in a tryptophane-2,3-dioxygenase model reaction with **1** as the catalyst much faster in DCM than in DMF.[8] No explanation for these obvious effects of the solvent on oxygenation reactions with **1** has yet been provided.

Several important steps of the overall reaction have, however, been identified, among them the formation of 1:1 and 1:2 aggregates of O_2 and Co(salen),[4,18] displacement of a solvent molecule by O_2 in Co(salen) analogues,[19,20] involvement of Co^{III}(salen)−substrate[21] or ternary complexes composed of the Co(salen) unit, O_2, and the substrate,[22,23] and, most important, electron transfer[22,24,25] (ET).

ET reactions of **1** have been intensively studied (for a recent review of some aspects, see ref 25). The oxidation of the neutral Co(II) chelate to the ionic Co(III) complex **1**$^+$ is quasi-reversible.[26−28] The formal potential E^0 for this process strongly depends on the solvent,[28,29] and is linearly correlated to the donor

† E-mail: bs@echem3.orgchemie.chemie.uni-tuebingen.de.

⊗ Abstract published in *Advance ACS Abstracts,* June 15, 1997.

(1) For part 2, see ref 35.
(2) Tsumaki, T. *Bull. Chem. Soc. Jpn.* **1938**, *13*, 252−260.
(3) Bailes, R. H.; Calvin, M. *J. Am. Chem. Soc.* **1947**, *69*, 1886−1893.
(4) Niederhoffer, E. C.; Timmons, J. H.; Martell, A. E. *Chem. Rev.* **1984**, *84*, 137−203.
(5) Matsuura, T. *Tetrahedron* **1977**, *33*, 2869−2905.
(6) Bolzacchini, E.; Brambilla, A. M.; Orlandi, M.; Rindone, B. *Life Chem. Rep.* **1995**, *13*, 71−77.
(7) Aimoto, Y.; Kanda, W.; Meguro, S.; Miyahara, Y.; Ōkawa, H.; Kida, S. *Bull. Chem. Soc. Jpn.* **1985**, *58*, 646−650.
(8) Nishinaga, A.; Ohara, H.; Tomita, H.; Matsuura, T. *Tetrahedron Lett.* **1983**, *24*, 213−216.
(9) Nishinaga, A.; Tsutsui, T.; Moriyama, H.; Wazaki, T.; Mashino, T.; Fujii, Y. *J. Mol. Catal.* **1993**, *83*, 117−123.
(10) Nishinaga, A.; Tojo, T.; Matsuura, T. *J. Chem. Soc., Chem. Commun.* **1974**, 896−897.
(11) Benedini, F.; Galliani, G.; Nali, M.; Rindone, B.; Tollari, S. *J. Chem. Soc., Perkin Trans. 2* **1985**, 1963−1967.
(12) Nishinaga, A.; Yamazaki, S.; Matsuura, T. *Tetrahedron Lett.* **1988**, *29*, 4115−4118.
(13) Nishinaga, A.; Förster, S.; Eichhorn, E.; Speiser, B.; Rieker, A. *Tetrahedron Lett.* **1992**, *33*, 4425−4428.
(14) Förster, S.; Rieker, A.; Maruyama, K.; Murata, K.; Nishinaga, A. *J. Org. Chem.* **1996**, *61*, 3320−3326.
(15) Nali, M.; Rindone, B.; Tollari, S.; Valletta, L. *J. Mol. Catal.* **1987**, *41*, 349−354.
(16) Bassoli, A.; Di Gregorio, G.; Rindone, B.; Tollari, S.; Chioccara, F.; Salmona, M. *Gazz. Chim. Ital.* **1988**, *118*, 763−768.
(17) Vol'pin, M. E.; Novodarova, G. N. *J. Mol. Catal.* **1992**, *74*, 153−162.
(18) Jones, R. D.; Summerville, D. A.; Basolo, F. *Chem. Rev.* **1979**, *79*, 139−179.
(19) Zhang, M.; van Eldik, R.; Espenson, J. H.; Bakac, A. *Inorg. Chem.* **1994**, *33*, 130−133.
(20) Rybak-Akimova, E. V.; Masarwa, M.; Marek, K.; Warburton, P. R.; Busch, D. H. *J. Chem. Soc., Chem. Commun.* **1996**, 1451−1452.
(21) Nishinaga, A.; Kuwashige, T.; Tsutsui, T.; Mashino, T.; Maruyama, K. *J. Chem. Soc., Dalton Trans.* **1994**, 805−810.
(22) Basolo, F. In *Facets of Coordination Chemistry*; Agarvala, B. V., Munshi, K. N., Eds.; World Scientific: Singapore, **1993**; pp 24−45.
(23) Hiller, W.; Nishinaga, A.; Rieker, A. *Z. Naturforsch.* **1992**, *47b*, 1185−1188.
(24) Carter, M. J.; Rillema, D. P.; Basolo, F. *J. Am. Chem. Soc.* **1974**, *96*, 392−400.
(25) Costa, G.; Tavagnacco, C. *Gazz. Chim. Ital.* **1995**, *125*, 243−261.
(26) Kapturkiewicz, A.; Behr, B. *Inorg. Chim. Acta* **1983**, *69*, 247−251.
(27) Kapturkiewicz, A.; Behr, B. *J. Electroanal. Chem.* **1984**, *163*, 189−198.
(28) Kapturkiewicz, A.; Behr, B. *J. Electroanal. Chem.* **1984**, *179*, 187−199.
(29) Reisenhofer, E.; Costa, G. *Inorg. Chim. Acta* **1981**, *49*, 121−124.

S0020-1669(97)00333-9 CCC: $14.00

Scheme 1. Three-Rung Ladder Scheme for Redox and Ligand Exchange Reactions at Co(salen)

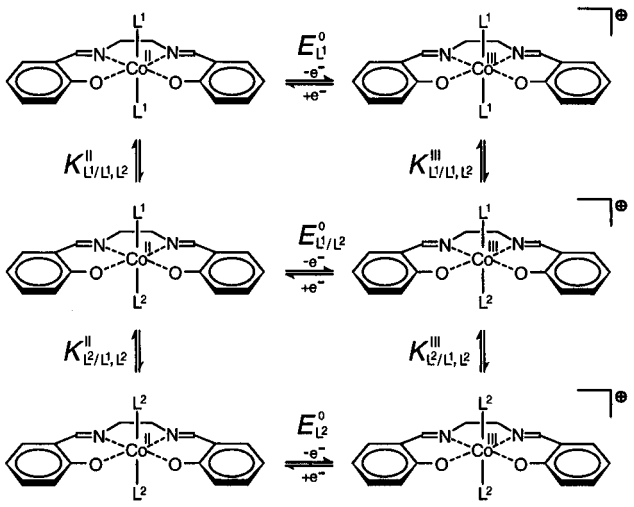

number of the solvent. Stronger donor solvents shift E^0 to more negative potentials, making the Co(II) complex easier to oxidize. Although this suggests the involvement of the solvent in the overall electrode process,[29] a molecular explanation of the interaction between **1** and the solvent molecules has not been proposed. Such an interaction, however, might be one of the crucial factors affecting oxygen transfer to the substrate. Electrochemical experiments in solvent mixtures, on the other hand, have qualitatively shown that *two* solvent molecules are axially associated to the central cobalt atom in both Co(II) and Co(III) forms of the chelate.[30] A three-rung ladder scheme[31] (Scheme 1)[32] was formulated to explain the changes in cyclic voltammetric curve shapes as a function of the solvent composition.

The present manuscript reports a complete thermodynamic analysis of this ladder scheme in the solvent system L^1 = DMF/L^2 = py (py = pyridine) with quantitative characterization of all three E^0 and four K from electrochemical and UV/vis spectroscopic experiments as well as the construction of thermodynamic cycles. Thus, the basic reaction possibilities of **1** and $\mathbf{1}^+$ in DMF/py mixtures are defined.[33] The solvent exchange provides a model for the substitution of solvent by substrate or O_2 molecules.[19,20,34]

Experimental Section

Preparation of the Co Complexes. Co(salen) was synthesized by following Bailes and Calvin.[3] The preparation of Co^{III}(salen)Cl, $[Co^{III}(salen)(DMF)]_2^+[ClO_4]^-$, and $[Co^{III}(salen)(DMF)]_2^+[PF_6]^-$ was described earlier.[35,36]

(*N,N′*-bis(salicylidene)ethylenediaminato)cobalt(III) perchlorate bishydrate, $[Co^{III}(salen)(H_2O)_2]^+[ClO_4]^-$, was synthesized from 0.50 g (1.46 mmol) of Co(salen)OH (prepared according to ref 2), dissolved in 5 mL of MeOH. After addition of 1 equiv of perchloric acid (130 μL of 70% $HClO_4$ in water) a precipitate formed which was, however, difficult to separate by filtration. Its suspension was poured into 50 mL of ethyl acetate and stirred for 5 min. The crystalline product was separated. Drying *in vacuo* yielded 440 mg (71%) of $[Co^{III}(salen)(H_2O)_2]^+[ClO_4]^-$. *Although no problems were encountered, it should be noted that perchlorate complexes in general may be explosive and should be handled with due care.* The ^{1}H-NMR spectrum in DMF was identical to that of the bis-DMF complex,[36] but showed an enhanced water peak. ^{13}C-CP-MAS solid-state NMR spectrum: δ = 59.9 ppm (s, ethylene bridge), 115.7−136.6 ppm (aromatic ring), 152.1−163.9 ppm (aromatic C bound to O), 172.0 (s, azomethine C). Anal. Calcd for $C_{16}H_{14}ClCoN_2O_6\cdot 2H_2O$ (460.71): C, 41.71; H, 3.94; N, 6.08; Cl, 7.69. Found: C, 41.43; H, 4.07; N, 6.14; Cl, 6.99.

Solvents and Supporting Electrolytes. DMF was distilled over P_2O_5 and subsequently fractionated three times under nitrogen at a pressure of 10 Torr in a packed column (length: 0.5 m). Each time the first 25% of the distillate and a residue of 10% were discarded. All distillations were performed with exclusion of light. Under a nitrogen atmosphere and in the dark, the DMF thus purified can be stored a few days without decomposition. Care was taken to remove basic impurities which coordinate to the Co(III) complexes and cause additional reduction peaks in the voltammograms.

py was stored over KOH and distilled under nitrogen immediately before use.

The supporting electrolyte $[NBu_4][PF_6]$ was synthesized[37] from $[NBu_4]Br$ and $[NH_4][PF_6]$ (both Fluka, Buchs, Switzerland). Alternatively, recycled supporting electrolyte[37] was used.

General Procedures for Cyclic Voltammetry. Cyclic voltammograms (CVs) were recorded with a combination of a Bruker Polarograph E310, a Wenking function generator VSG72, and a Houston Omnigraphic 2000 recorder, with a BAS 100B electrochemical analyzer or a BAS 100B/W electrochemical workstation of Bioanalytical Systems. The working electrode was a Pt electrode tip (BAS or Metrohm; electroactive area A = 0.068 or 0.076 cm^2), while a Pt wire served as the counter electrode. A $Ag/AgClO_4$ (0.01 M in $[NBu_4][PF_6]/CH_3CN$) electrode was used as reference and separated by two glass frits from a Haber-Luggin capillary. Ferrocene (fc) served as external standard. Its cyclic voltammograms were recorded versus the silver reference electrode in all solvent mixtures used. All potential values determined (E_{Ag/Ag^+}) were then rescaled to $E^0(fc/fc^+)$ [fc^+ is the ferrocenium ion; $E^0(fc/fc^+) = (E_p^{ox} + E_p^{red})/2$ from the fc voltammograms; $E_{fc/fc^+} = E_{Ag/Ag^+} - E^0(fc/fc^+)$] in the respective solvent and are given versus this standard[38] in the present paper.

Most experiments were performed in a vacuum-tight full-glass cell under an atmosphere of nitrogen or argon. The electrolyte (0.1 M $[NBu_4]^+[PF_6]^-$ in the respective solvent) was saturated with the inert gas and filled into the cell under a counter current of nitrogen or argon. Between two cyclic voltammetric experiments nitrogen or argon gas saturated with the solvent vapor was bubbled through the electrolyte. Alternatively, the electrolyte was degassed by freeze−pump−thaw cycles prior to the experiment and transferred into the cell under argon.[37]

Simulation of Cyclic Voltammograms. Theoretical current−potential curves were generated with the simulation program CVSIM from our EASI package[39] by means of spline orthogonal collocation[40] and the expanding simulation space model[41] or with the commercial DigiSim program[42] (FIFD algorithm, default numerical options).

UV/Vis Spectra. Stock solutions with a concentration [**1**] = 0.125 mM in DMF and py were prepared under a nitrogen atmosphere, filled into nitrogen purged cuvettes (path length 1 cm) in defined volumes, and mixed. Extinctions were recorded in 5 nm steps with a Spectronic 20 spectral photometer (Milton Roy). As a reference the solvent mixtures without **1** were used.

(30) Eichhorn, E.; Rieker, A.; Speiser, B. *Angew. Chem.* **1992**, *104*, 1246−1248; *Angew. Chem., Int. Ed. Engl.* **1992**, *31*, 1215−1217.
(31) Evans, D. H. *Chem. Rev.* **1990**, *90*, 739−751.
(32) The subscripts in the E^0 in Scheme 1 denote the solvent molecules attached to the Co central atom in both partners of the redox couple. The superscripts in the K symbolize the oxidation state of the central Co atom; the first part of the subscripts defines the fixed solvent molecule, while the second and third show the two exchanging ligands, arranged in the order of increasing basicity. The exchanging solvent molecules have been omitted from the equilibrium arrows in the scheme.
(33) **1** and $\mathbf{1}^+$ will be used as a generic notation for the Co(II) and Co(III) salen complexes. If reference is made to complexes with specific axial ligands, a notation such as Co(salen)(L^1)(L^2) will be used.
(34) Speiser, B.; Stahl, H. *Angew. Chem.* **1995**, *107*, 1222−1224; *Angew. Chem., Int. Ed. Engl.* **1995**, *34*, 1086−1089.
(35) Eichhorn, E.; Rieker, A.; Speiser, B.; Sieglen, J.; Strähle, J. *Z. Naturforsch.* **1993**, *48b*, 418−424.
(36) Gollas, B.; Speiser, B.; Stahl, H.; Sieglen, J.; Strähle, J. *Z. Naturforsch.* **1996**, *51b*, 388−398.
(37) Dümmling, S.; Eichhorn, E.; Schneider, S.; Speiser, B.; Würde, M. *Curr. Sep.* **1996**, *15*, 53−56.
(38) Gritzner, G.; Kůta, J. *Pure Appl. Chem.* **1984**, *56*, 461−466.
(39) Speiser, B. *Comput. Chem.* **1990**, *14*, 127−140.
(40) Hertl, P.; Speiser, B. *J. Electroanal. Chem.* **1988**, *250*, 237−256.
(41) Urban, P.; Speiser, B. *J. Electroanal. Chem.* **1988**, *241*, 17−31.
(42) Rudolph, M.; Reddy, D. P.; Feldberg, S. W. *Anal. Chem.* **1994**, *66*, 589A−600A.

Table 1. Thermodynamic Parameters of Ladder Scheme 1 with L^1 = DMF and L^2 = py

quantity	value	n^a	ΔG^0/J mol^{-1} [b]	ΔG^0/J mol^{-1} [c]	remarks
E^0_{DMF}	-0.465 ± 0.005 V	1500	$-(4.48 \pm 0.05) \times 10^4$	$-44\,770 \pm 480$	*d*, *h*
E^0_{py}	-0.874 ± 0.005 V	78	$-(8.43 \pm 0.05) \times 10^4$	$-84\,330 \pm 480$	*d*, *h*
$E^0_{DMF/py}$	-0.629 ± 0.008 V	73	$-(6.07 \pm 0.08) \times 10^4$	$-60\,690 \pm 770$	*d*, *h*
$K^{II}_{DMF/DMF,py}$	58 ± 18	270	$-(1.01^{+0.07}_{-0.1}) \times 10^4$	$-10\,055^{+920}_{-670}$	*e*
$K^{II}_{py/DMF,py}$	0.85 ± 0.3	65	$+(0.4^{+0.7}_{-1.1}) \times 10^2$	$+400^{+750}_{-1080}$	*d*
$K^{III}_{DMF/DMF,py}$	$(4.0 \pm 0.6) \times 10^4$	98	$-(2.62^{+0.03}_{-0.04}) \times 10^4$	$-26\,240^{+420}_{-360}$	*d*
$K^{III}_{py/DMF,py}$	$(1.2^{+0.7}_{-0.4}) \times 10^4$	–	$-(2.3^{+0.14}_{-0.12}) \times 10^4$	$-23\,240^{+1154}_{-1385}$	*f*
$K^{III}_{py/DMF,py}$	$(1.1^{+0.7}_{-0.5}) \times 10^4$	–	$-(2.3^{+0.16}_{-0.13}) \times 10^4$	$-22\,975^{+1600}_{-1280}$	*g*

[a] Number of experimental determinations used for the calculation, "–" indicates indirect determination via thermodynamic cycle. [b] Rounded values. Error measure: standard deviation σ. [c] Exact values as calculated from the corresponding mean of E^0 or K. Error measure: standard deviation σ. [d] From cyclic voltammograms. [e] From UV/vis spectrophotometry. [f] Calculated via thermodynamic cycle B. [g] Calculated via thermodynamic cycle C. [h] Referred to E^0(fc/fc$^+$); ΔG^0 is Gibbs free energy of reaction Co(II) + fc$^+$ ⇌ Co(III)$^+$ + fc; Co(III) complexes are regarded as products.

Results[43]

Parameters from Electroanalytical Experiments. The thermodynamic parameters E^0_{DMF}, E^0_{py}, $E^0_{DMF/py}$, $K^{II}_{py/DMF,py}$, and $K^{III}_{DMF/DMF,py}$ were determined from cyclic voltammograms of **1** or its one-electron oxidation products $\mathbf{1}^+X^-$ ($X^- = Cl^-$, $[ClO_4]^-$, $[PF_6]^-$). Both, the bis(water) and the bis-DMF perchlorate of $\mathbf{1}^+$ were used with essentially identical results.

Determination of E^0_{DMF} and E^0_{py}. The formal potentials of the Co complexes bearing two identical axial solvent molecules were determined as the midpoint potentials $\bar{E} = (E^{ox}_p + E^{red}_p)/2$ in cyclic voltammograms of **1**, $\mathbf{1}^+Cl^-$ (see ref 35), $\mathbf{1}^+[ClO_4]^-$, or $\mathbf{1}^+[PF_6]^-$ (see refs 36 and 44) recorded in the plain solvents. Mean values of E^0_{DMF} and E^0_{py} are given in Table 1.

In the presence of only a single basic species, either DMF or py, redox reactions 1 or 2 occur at the electrode.

$$Co^{II}(salen)(DMF)_2 \overset{E^0_{DMF}}{\rightleftharpoons} [Co^{III}(salen)(DMF)_2]^+ + e^- \quad (1)$$

$$Co^{II}(salen)(py)_2 \overset{E^0_{py}}{\rightleftharpoons} [Co^{III}(salen)(py)_2]^+ + e^- \quad (2)$$

In accordance with earlier results,[26–28,35,36,45–51] in all cases the Co(II)/Co(III) redox couple exhibits quasi-reversible one-electron redox behavior (E_{qr} mechanism; peak potential difference $\Delta E_p > 58$ mV, increasing with scan rate υ; data in Supporting Information, Table S1). The extent of quasi-reversibility critically depends on the history of the electrode surface. In particular, the electrode was polished frequently between scans to prevent the continuous loss of electrode activity with time and to improve reproducibility of repeated ΔE_p determinations.

Typical experimental cyclic voltammograms for various υ were simulated under the assumption of an E_{qr} mechanism.[52] Both simulation programs used, DigiSim and CVSIM, generated almost identical results (Figure 1). Slight differences between the DigiSim and the CVSIM curves result from the consideration of uncompensated resistance in the DigiSim simulations (R_u = 30 Ω, determined with the BAS 100B). Values for the apparent heterogeneous ET rate constant k_s and the transfer coefficient α were determined from fitting entire voltammograms (DigiSim) or from the multiparameter estimation technique implemented in the EASI program package.[53,54] ET kinetics in both DMF and py are characterized by $0.01 > k_s > 0.005$ cm s^{-1} with α deviating only slightly from 0.5. The peak current ratio,[55] i^{red}_p/i^{ox}_p (for **1**) or i^{ox}_p/i^{red}_p (for $\mathbf{1}^+$), was near unity (see Table S1), indicating that chemical reactions coupled to the ET are not important.

Additionally, in all voltammograms evaluated in this work, $|E_\lambda - \bar{E}|$ was at least 300 mV. Thus, the midpoint potential $\bar{E}$ provides an estimate[56] of E^0.

Quasi-reversibility may unsymmetrically shift the peak potentials from E^0 if k_s is small and α deviates from 0.5. For $k_s > 0.002$ cm s^{-1} as in the present case, however, the deviation of $\bar{E}$ from E^0 is often assumed to be negligible.[57] Furthermore, the shifts of E^{ox}_p and E^{red}_p increase with increasing υ. Consequently, if observable, any deviation between $\bar{E}$ and E^0, and, concomitantly, a shift of $\bar{E}$, would increase with υ. In the evaluation presented here, only experiments were considered where $\bar{E}$ did not vary more than 15 mV in the range 0.05 V s^{-1} < υ < 1 V s^{-1}. Usually, however, the apparent quasi-reversibility of redox reactions 1 and 2 did influence $\bar{E}$ much less.

The diffusion coefficients of $Co^{II}(salen)(DMF)_2$ and $[Co^{III}(salen)(DMF)_2]^+$ in DMF slightly differ.[36,52] Such a difference

(43) The following definitions will be used throughout this manuscript. In all solvent exchange equilibria the complex carrying the higher number of DMF molecules will be regarded as the *educt*; the complex containing the higher number of py ligands is the *product*. Reaction 18

$$Co^{II/III}(salen)(DMF)_2^{0/+} + py \rightleftharpoons Co^{II/III}(salen)(DMF)(py)^{0/+} + DMF \quad (18)$$

will be denoted as the *first*, and reaction 19

$$Co^{II/III}(salen)(DMF)(py)^{0/+} + py \rightleftharpoons Co^{II/III}(salen)(py)_2^{0/+} + DMF \quad (19)$$

as the *second* solvent exchanges in either oxidation state. Other general definitions are given in note 32.

(44) Eichhorn, E.; Speiser, B. *J. Electroanal. Chem.* **1994**, *365*, 207–212.
(45) Higson, B. M.; McKenzie, E. D. *Inorg. Nucl. Chem. Lett.* **1970**, *6*, 209–213.
(46) Rohrbach, D. F.; Deutsch, E.; Heineman, W. R. In *Characterization of Solutes in Nonaqueous Solvents*; Mamantov, G., Ed.; Plenum: New York, 1978; pp 177–195.
(47) Rohrbach, D. F.; Heineman, W. R.; Deutsch, E. *Inorg. Chem.* **1979**, *18*, 2536–2542.
(48) Hanzlik, J.; Puxeddu, A.; Costa, G. *J. Chem. Soc., Dalton Trans.* **1977**, 542–546.
(49) Kitaura, E.; Nishida, Y.; Ōkawa, H.; Kida, S. *J. Chem. Soc., Dalton Trans.* **1987**, 3055–3059.
(50) Averill, D. F.; Broman, R. F. *Inorg. Chem.* **1978**, *17*, 3389–3394.
(51) Costa, G.; Mestroni, G.; Puxeddu, A.; Reisenhofer, E. *J. Chem. Soc. A* **1970**, 2870–2874.
(52) General parameters for the simulations: $A = 0.076$ cm^2, $E^0 = -0.445$ V. Parameters used in simulations of voltammograms of **1**: $D = 5.3 \times 10^{-6}$ cm^2 s^{-1}, $k_s = 0.007$ cm s^{-1}, $\alpha = 0.65$. Parameters used in simulations of voltammograms of $\mathbf{1}^+$: $D = 3.8 \times 10^{-6}$ cm^2 s^{-1}, $k_s = 0.009$ cm s^{-1}, $\alpha = 0.42$.
(53) Speiser, B. *Anal. Chem.* **1985**, *57*, 1390–1397.
(54) Scharbert, B.; Speiser, B. *J. Chemomet.* **1988**, *3*, 61–80.
(55) Nicholson, R. S. *Anal. Chem.* **1966**, *38*, 1406.
(56) Nicholson, R. S.; Shain, I. *Anal. Chem.* **1964**, *36*, 706–723.
(57) Paul, H. J.; Leddy, J. *Anal. Chem.* **1995**, *67*, 1661–1668.

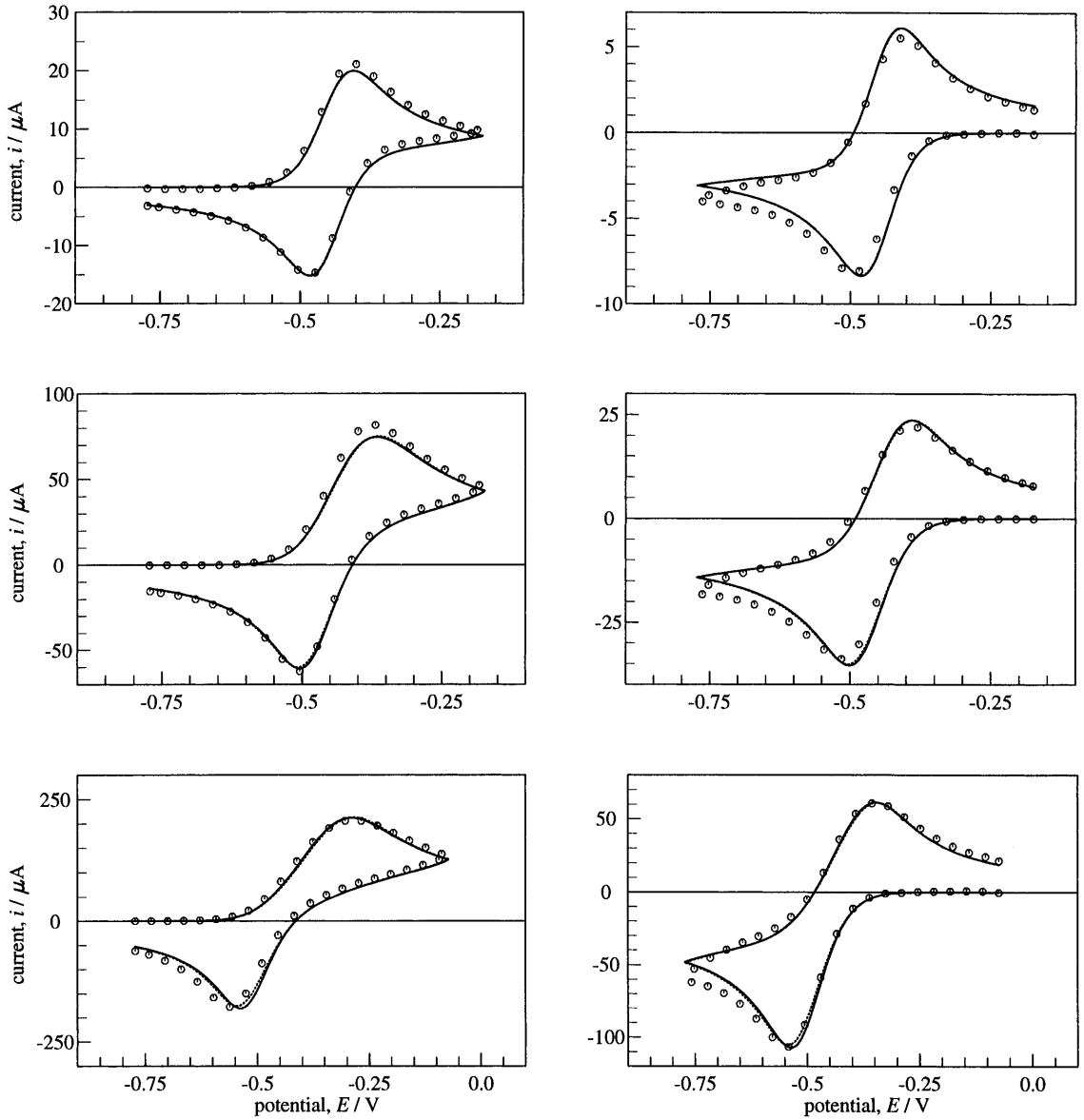

Figure 1. Experimental (symbols) and simulated (lines: full, CVSIM; broken, DigiSim) cyclic voltammograms of **1** (left, $c = 2.06$ mM) and $\mathbf{1}^+$ (as perchlorate, right, $c = 0.96$ mM) in DMF. Parameters are as in note 52. From top to bottom, $v = 0.05$, 1.0, and 10.24 V s^{-1}.

shifts[58] $E_{1/2}$ from E^0. In the present system the deviation is estimated to be <4 mV, well within the reproducibility of the experimental determination of $\bar{E}$.

To allow comparison of the formal potentials in DMF and py, all potential values are referred to $E^0(fc/fc^+)$ in the respective solvent (see Experimental Section). The fc/fc^+ couple has been proposed as a solvent independent potential standard.[38]

Determination of $K^{II}_{py/DMF,py}$. If DMF is added to solutions of **1** in py (DMF mole fraction $x_{DMF} < 0.95$), the quasi-reversible shape of the cyclic voltammograms is retained. The peaks, however, shift to more positive potentials (Figure 2a). Analogous results with a shift in the opposite direction are obtained if py is added to solutions of **1** in DMF as long as $x_{DMF} < 0.95$. The resulting variation of $\bar{E}$ [referred to $E^0(fc/fc^+)$ in the respective solvent mixture] is a continuous but nonlinear function of x_{DMF} (Figure 2b, circles). Only for $x_{DMF} > 0.95$ the oxidation peak starts to change its shape, and the reduction signal splits into several peaks.[30,44]

We explain the peak shift for $x_{DMF} < 0.95$ by a chemical pre-equilibrium coupled to the Co(II)/Co(III) ET. If py is present in a large excess over **1**, ladder Scheme 1 reduces to reaction 3 (CE mechanism). Before the voltammetric scan

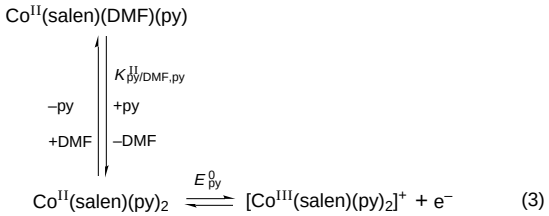

begins, an equilibrium between $Co^{II}(salen)(DMF)(py)$ and $Co^{II}(salen)(py)_2$ is established. Of these two complexes, the bis-py form is more easily oxidized. The cationic complex $[Co^{III}(salen)(py)_2]^+$ is formed, while $Co^{II}(salen)(py)_2$ is replenished by substitution of DMF with py from $Co^{II}(salen)(DMF)(py)$. If this equilibrium is maintained quickly, all Co(II) complex is oxidized via reaction 3, and only a single oxidation peak is observed.

$[Co^{III}(salen)(py)_2]^+$ is that Co(III) complex in ladder Scheme 1 which is most difficult to reduce. Still, on the reverse scan of the voltammogram, we only observe the reduction of this species. Only for larger DMF concentrations ($x_{DMF} > 0.95$) reduction signals of the other two Co(III) complexes appear,

(58) In ref 80, p 158.

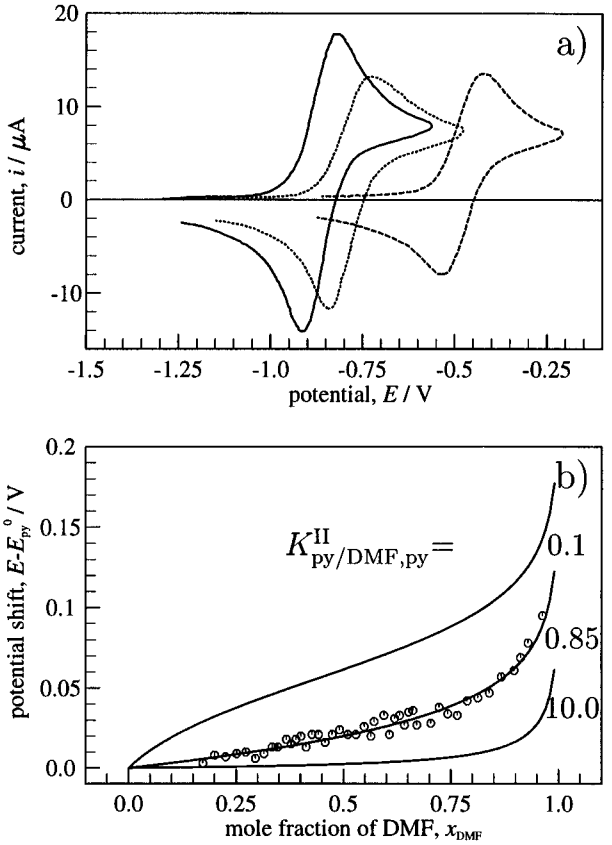

Figure 2. Peak shift in cyclic voltammograms of **1** in DMF/py mixtures: (a) cyclic voltammograms in py (—; c = 1.27 mM), DMF (- - -; c = 1.05 mM), and mixture with x_{DMF} = 0.926 (···; c = 0.97 mM); (b) shift of midpoint potentials $\bar{E} \approx E^0$, (○) experimental values, (lines) calculated dependence on x_{DMF} according to eq 6 with $K^{II}_{py/DMF,py}$ = 0.1, 0.85, and 10.0.

one after the other. Thus, the ligand exchange equilibria in the Co(III) state are very much in favor of the bis-py species (see species distribution diagrams, below) and the exchange reactions in the Co(III) species are very slow. For $x_{DMF} < 0.95$, the influence of the Co(III) equilibria on the voltammograms is negligible.

Reversible CE reactions with an equilibrium composed of first-order forward and reverse reactions have been simulated for voltammetric conditions,[56,59] and, accordingly, the midpoint potential for a primary oxidative ET is given by

$$\bar{E} = E^0 - \frac{RT}{F}\ln\left(\frac{K'}{1+K'}\right) \tag{4}$$

where K' is the equilibrium constant for the pre-equilibrium. Under our conditions, both DMF and py are present in a large excess over **1**, and the equilibrium in reaction 3 consists of pseudo-first order reactions. It is described by

$$K^{II}_{py/DMF,py} = \frac{[Co^{II}(salen)(py)_2][DMF]}{[Co^{II}(salen)(DMF)(py)][py]} = K^{II'}_{py/DMF,py}\frac{[DMF]}{[py]} = K^{II'}_{py/DMF,py}\frac{x_{DMF}}{1-x_{DMF}} \tag{5}$$

with $K^{II'}_{py/DMF,py} = [Co^{II}(salen)(py)_2]/[Co^{II}(salen)(DMF)(py)]$,

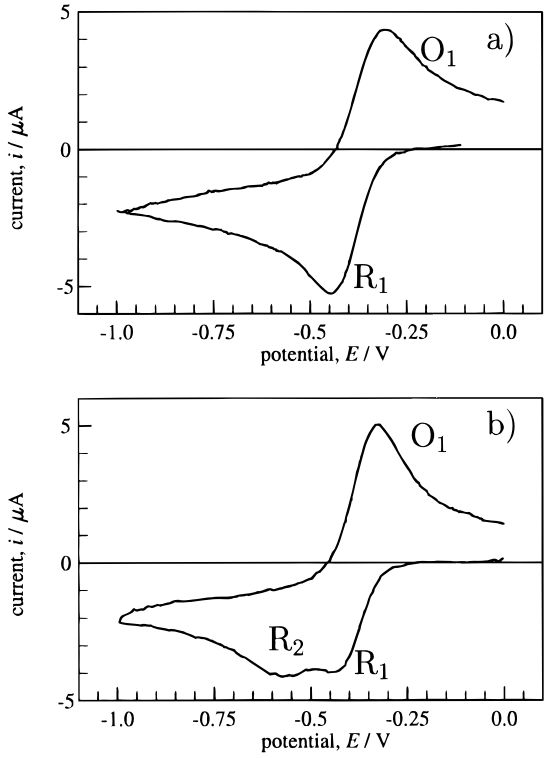

Figure 3. Cyclic voltammograms of $\mathbf{1}^+$ in DMF ($[Co^{III}]^0$ = 0.225 mM) (a) before and (b) after after addition of py ($[py]^0$ = 0.225 mM), υ = 0.5 V s^{-1}.

and thus,

$$\bar{E} = E^0_{py} - \frac{RT}{F}\ln\left(\frac{K^{II}_{py/DMF,py}[py]/[DMF]}{1+K^{II}_{py/DMF,py}[py]/[DMF]}\right) = E^0_{py} - \frac{RT}{F}\ln\left(\frac{K^{II}_{py/DMF,py}(1-x_{DMF})}{x_{DMF}+K^{II}_{py/DMF,py}(1-x_{DMF})}\right) \tag{6}$$

A best fit between experimental $\bar{E}$ values for **1** in DMF/py mixtures as a function of x_{DMF} and curves calculated from eq 6 is obtained for $K^{II}_{py/DMF,py}$ = 0.85 (Figure 2b; see also Supporting Information, Table S2). It appeared essential to refer $\bar{E}$ to $E^0(fc/fc^+)$ in the respective solvent composition to obtain consistent $K^{II}_{py/DMF,py}$ values.

It was supposed that the exchange equilibrium is fast in the time scale of the experiments. Indeed, no appreciable effect of υ on $\bar{E}$ is observed. Only a single oxidation peak is found, which additionally confirms this assumption: If the exchange of axial ligands in the Co(II) oxidation state were slow, oxidation signals of the other Co(II) complexes were expected. Furthermore, we assumed that the first solvent exchange in the Co(II) oxidation state does not obscure the data. Such an additional coupled equilibrium would contribute to the shift of $\bar{E}$, and a systematic variation of $K^{II}_{py/DMF,py}$ with the solvent composition was expected. This is indeed observed but only for $x_{DMF} > 0.98$ (see Supporting Information, Table S2), and data from this range of the solvent composition were excluded from the analysis.

Finally, a possible effect of the apparent quasi-reversibility of the Co(II)/Co(III) ET in the bis-py form on $\bar{E}$ was neglected. This was supported by simulation results for the CE_{qr} reaction in accordance with earlier reports.[60] In particular, the behavior of $\bar{E}$ as a function of k_s and α was analyzed, when the rate

(59) Savéant, J. M.; Vianello, E. *Compt. Rend. Acad. Sci. Paris* **1963**, *256*, 2597−2600.

(60) Moulton, R. D.; Bard, A. J.; Feldberg, S. W. *J. Electroanal. Chem.* **1988**, *256*, 291−307.

constants of the equilibrium reactions were high, as corresponds to our case. For $\alpha = 0.5$, $\bar{E}$ follows eq 6 closely, even for small k_s, due to the symmetrical shift of the two peaks with respect to E^0. On the other hand, for $\alpha \neq 0.5$, $\bar{E}$ deviates from eq 6 progressively with decreasing k_s and increasing shift of the pre-equilibrium to the side of the nonelectroactive species. We also analyzed such simulated $\bar{E}$ values with eq 6, and the resulting values of the equilibrium constant showed a systematic drift as a function of solvent composition. Such a variation was not observed in the experimental data for **1**, and we conclude that the apparent quasi-reversibility of the Co(II)/Co(III) ET does not disturb the calculation of $K^{II}_{py/DMF,py}$.

Determination of $K^{III}_{DMF/DMF,py}$. In DMF, $\mathbf{1}^+$ shows a single peak couple (R_1, O_1) at E^0_{DMF} in cyclic voltammograms due to redox reaction 1 (Figure 3a). Similarly, in py, a peak couple at E^0_{py} is observed at a more negative potential (reaction 2). If we add py to a solution of $\mathbf{1}^+$ in DMF in concentrations lower or only slightly larger than the concentration of the complex, two reduction signals R_1 and R_2 appear (Figure 3b). At somewhat higher concentrations of py, a third reduction peak is found.[30] Peaks R_1 and R_2 are attributed to the reduction of $[Co^{III}(salen)(DMF)_2]^+$ and $[Co^{III}(salen)(DMF)(py)]^+$, respectively. Under the conditions mentioned, ladder Scheme 1 reduces to its upper square scheme, i.e. reaction 7. Only a single

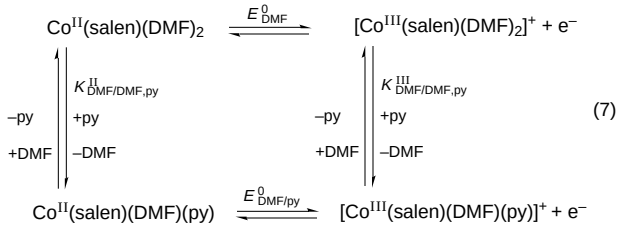

(7)

oxidation peak O_1 is observed,[44] which indicates that the equilibrium in the Co(II) oxidation state of reaction scheme 7 is very fast and shifted to the side of $Co^{II}(salen)(DMF)_2$. In multicycle voltammograms isopotential points[61] occur,[44] and hence, no side reactions lead out of the square scheme.

At the beginning of the voltammetric scan, the solvent exchange reaction for the Co(III) complexes in reaction scheme 7 is in equilibrium and $[Co^{III}(salen)(DMF)_2]^+$ and $[Co^{III}(salen)(DMF)(py)]^+$ have concentrations determined by $K^{III}_{DMF/DMF,py}$.

For scan rates $v > 0.5$ V s^{-1} the ratio of peak currents $i_p^{R_2}/i_p^{R_1}$ becomes essentially independent of v. The relaxation of the equilibrium on the right-hand side of reaction 7 is slow, as usually observed for ligand substitution reactions at Co(III).[62] In these faster time scales, the equilibrium can no longer follow changes of concentrations due to ET at the electrode, and the proportionality of peak currents to concentrations was used to determine the concentration ratio of the two Co(III) species in solution. Two approaches were used to calculate

$$K^{III}_{DMF/DMF,py} = \frac{[[Co^{III}(salen)(DMF)(py)]^+][DMF]}{[[Co^{III}(salen)(DMF)_2]^+][py]} \quad (8)$$

at various $[Co^{III}]^0$ and ratios $[Co^{III}]^0/[py]^0$, where $[Co^{III}]^0$ indicates the total Co(III) complex concentration in solution

$$[Co^{III}]^0 = [[Co^{III}(salen)(DMF)(py)]^+] + [[Co^{III}(salen)(DMF)_2]^+] \quad (9)$$

and $[py]^0$ is the total py concentration.

Either $i_p^{R_1}$ and $i_p^{R_2}$ (referred to an appropriate baseline extrapolated from peak R_1) in the presence of py, or the decrease of $i_p^{R_1}$ upon addition of py to the DMF solution of $\mathbf{1}^+$, provided the necessary experimental information. Details of the procedures will be discussed elsewhere.[63] The mean value for $K^{III}_{DMF/DMF,py}$ is given in Table 1. Individual results for the equilibrium constant in each of the experiments can be found in the Supporting Information (Table S3). A first assumption used in this evaluation is that the addition of py to a DMF solution of the Co complex results in a decrease of the peak current proportional to the decrease in $[[Co^{III}(salen)(DMF)_2]^+]$ without changing the shape and position of reduction signal R_1. This is reasonable for the present situation, where the ET is quasi-reversible with a relatively large k_s, while the rate of the solvent exchange reactions is negligible.

Furthermore, for the first approach mentioned, we assume that the factors of proportionality between the concentrations of the two Co(III) species and the respective reduction currents are equal. This implies identical current functions for the two ETs and diffusion coefficients for the complexes, while the second evaluation does not rely on this assumption. The two approaches gave consistent results which indicates that indeed the assumption was fulfilled.

Finally, the second equilibrium in the Co(III) state is supposed to exert only negligible effects on the analysis. This assumption is verified by the fact that under the present conditions a third reduction peak [attributed to $[Co^{III}(salen)(py)_2]^+$] is not observed.

Determination of $E^0_{DMF/py}$. In contrast to the conditions for the determination of the thermodynamic parameters discussed above, it was not possible to find concentrations where either $Co^{II}(salen)(DMF)(py)$ or $[Co^{III}(salen)(DMF)(py)]^+$ were present in a large excess over the other two Co(II) or Co(III) complexes, respectively (see also species distribution diagrams, below).

According to Scheme 1, the quasi-reversible redox reaction of $[Co^{III}(salen)(DMF)(py)]^+$ is coupled to a follow-up reaction [substitution of py vs DMF in the Co(II) form]. Under conditions where mixed complexes can at all be observed, the high excess of DMF over both py and complex causes the ligand exchange to be essentially irreversible ($E_{qr}\underline{C}$ mechanism, reaction 10):

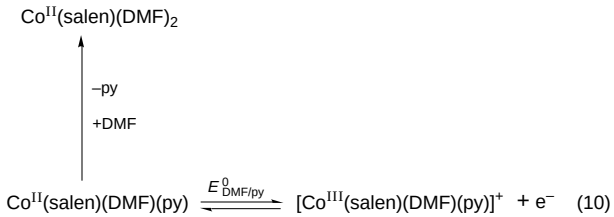

(10)

Formal potential $E^0_{DMF/py}$ (Table 1) was determined from a comparison of the experimental and simulated shift of $E_p^{R_2}$ with v, $[py]^0$, and $[Co^{III}]^0$.

Due to the absence of a reverse peak for the re-oxidation of $Co^{II}(salen)(DMF)(py)$ the rate constant k of the substitution reaction in the Co(II) ligand sphere was not accessible.[64] The reaction can, however, be assumed to be fast on the time scale of our experiments. Simulations of the $E_{qr}\underline{C}$ model by Evans[65] and calculations performed during this work consistently show that the ET is rate-limiting, and the peak potential in an $E_{qr}\underline{C}$

(61) Fitch, A.; Edens, G. J. *J. Electroanal. Chem.* **1989**, *267*, 1−13.
(62) In ref 81, p 732.
(63) Bee, U.; Eichhorn, E.; Rieker, A.; Speiser, B.; Stahl, H. Manuscript in preparation.
(64) From simulated two-cycle voltammograms of $\mathbf{1}^+$ in DMF/py we estimate $10^3 \leq k/\text{L mol}^{-1}\text{ s}^{-1} \leq 10^4$: Eichhorn, E.; Speiser, B.; et. al., manuscript in preparation.
(65) Evans, D. H. *J. Phys. Chem.* **1972**, *76*, 1160−1165.

Table 2. Comparison of Experimental Peak Potentials[a] $E^{R_2}_{p,exp}$ (Relative to the Peak Potential at $\upsilon = 0.05$ V s^{-1}) from Cyclic Voltammograms to Simulated Values from the $E_{qr}\underline{C}$ Mechanism

υ/V s^{-1}	$E^{R_2}_{p,exp}$/V	$E^{R_2}_{p,sim}$/V	υ/V s^{-1}	$E^{R_2}_{p,exp}$/V	$E^{R_2}_{p,sim}$/V
0.05	0.000	0.000	0.50	0.051	0.055
0.10	0.010	0.017	1.00	0.072	0.072
0.20	0.028	0.033	2.00	0.093	0.089

[a] Mean values over 9 experiments with $[Co^{III}]^0 = 0.25$, 0.50, and 1.00 mM, $[py]^0/[Co^{III}]^0 = 0.50$, 0.75, and 1.00.

system becomes independent of the follow-up reaction rate constant, if k is large. For example, for the k_s and α values in the present system, $E^{R_2}_p$ is expected to be independent of k if $k > 10^5$ s^{-1} ($\upsilon = 0.05$ V s^{-1}) or $k > 10^2$ s^{-1} ($\upsilon = 5.1$ V s^{-1}).

Comparison of experimental E^{R2}_p data to simulations with rate determining k_s shows good agreement (Table 2) and yields $E^0_{DMF/py}$.

For the above simulations, the heterogeneous ET rate constant for the mixed complex was set to k_s of the $Co^{II/III}(salen)(DMF)_2^{0/+}$ couple. The validity of this assumption could not be proven directly. We will, however, show below that the result for $E^0_{DMF/py}$ is well consistent with the other thermodynamic data.

Parameter from UV/Vis Spectroscopy. Determination of $K^{II}_{DMF/DMF,py}$. Electron spectra of **1** in the range $325 < \lambda < 530$ nm in pure DMF show two absorption maxima at $\lambda_1 = 350$ nm [ϵ_1(DMF) = 9500] and $\lambda_2 = 410$ nm [ϵ_2(DMF) = 10000] as well as a shoulder at $\lambda_3 = 460$ nm [ϵ_3(DMF) = 3000]. In py, the signals at λ_1 [ϵ_1(py) = 8000] and λ_3 [ϵ_3(py) = 3000] are still present while the maximum at λ_2 disappears. Spectra of **1** in mixtures of DMF and py with $1.0 \geq x_{DMF} \geq 0.9$ show a continuous decrease of the band at λ_2 with decreasing x_{DMF} (Figure 4a). For $x_{DMF} < 0.9$ the spectra change only slightly.

Due to the formation of bis-axially coordinated complexes in DMF/py as suggested by ladder Scheme 1 and by the electrochemical results, the spectrum in pure DMF is associated with $Co^{II}(salen)(DMF)_2$, while the one in pure py must be attributed to $Co^{II}(salen)(py)_2$. For $x_{DMF} > 0.9$ the second solvent exchange equilibrium is shifted far to the side of the mixed-solvated complex ($K^{II}_{py/DMF,py}$; see also species distribution diagrams, below). Consequently, the disappearance of the maximum at λ_2 is related to a shift in the first Co(II) exchange equilibrium in ladder Scheme 1, reaction 11:

$$Co^{II}(salen)(DMF)_2 + py \rightleftharpoons Co^{II}(salen)(DMF)(py) + DMF \quad (11)$$

In principle, the equilibrium constant

$$K^{II}_{DMF/DMF,py} = \frac{[Co^{II}(salen)(DMF)(py)][DMF]}{[Co^{II}(salen)(DMF)_2][py]} \quad (12)$$

is accessible from spectrophotometric experiments, if the spectrum of $Co^{II}(salen)(DMF)(py)$ is known. In analogy to the corresponding mixed Co(III) complex, however, we could not isolate this species, and in solution it is always mixed with one of the other Co(II) complexes. For $x_{DMF} \ll 0.9$, on the other hand, the concentration of $Co^{II}(salen)(DMF)_2$ becomes small. Only $Co^{II}(salen)(DMF)(py)$ and $Co^{II}(salen)(py)_2$ are present. They change their relative concentration with the solvent composition according to $K^{II}_{py/DMF,py}$. Knowledge of the latter equilibrium constant allows the construction of the mixed complex spectrum (Figure 4b). The spectra of $Co^{II}(salen)(DMF)(py)$ and $Co^{II}(salen)(py)_2$ appear to be rather similiar. The maximum in the latter is shifted to higher wavelengths by only about 10 nm, while the shoulder at $\lambda_3 = 460$ nm is slightly more pronounced for the mixed complex. The constructed spectrum of $Co^{II}(salen)(DMF)(py)$ forms the basis to calculate $K^{II}_{DMF/DMF,py}$ in solutions with $x_{DMF} \geq 0.9$. In the experiments the total Co(II) complex concentration $[Co^{II}]^0$ and the solvent composition were varied and the resulting values for the equilibrium constant (individual data in the Supporting Information, Table S5) were consistent (mean value in Table 1).

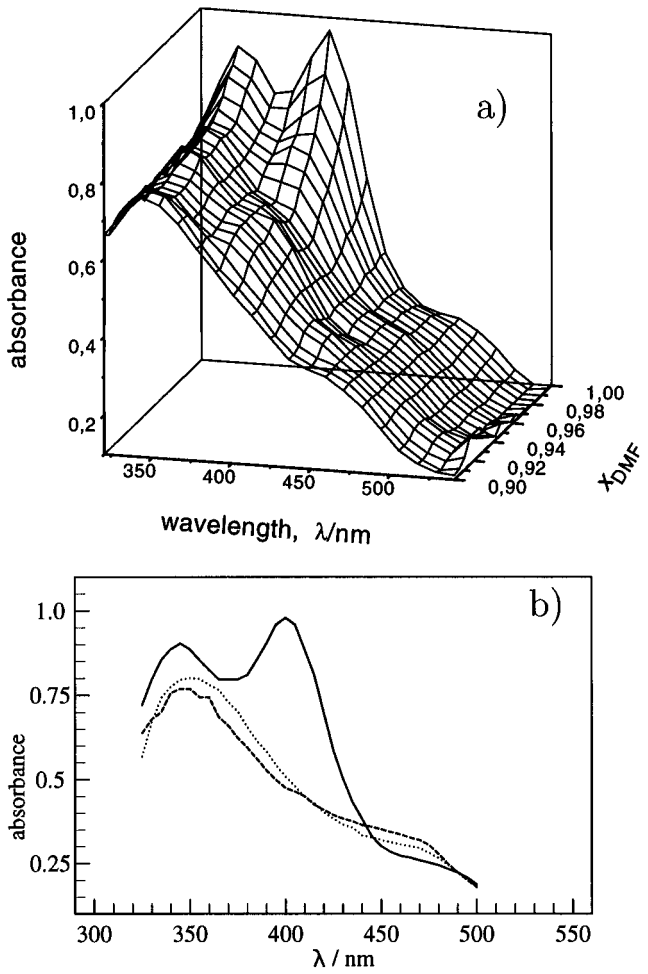

Figure 4. UV/vis absorption spectra of **1** in DMF/py: (a) dependence of spectra on solvent composition; (b) spectra of $Co^{II}(salen)(DMF)_2$ (solid line), $Co^{II}(salen)(DMF)(py)$ (calculated; broken line), and $Co^{II}(salen)(py)_2$ (dotted line); absorbance normalized to $[Co^{II}]^0 = 10^{-4}$ mM.

The spectra at $1.0 \geq x_{DMF} \geq 0.9$ show two isosbestic points at $\lambda = 440$ and $\lambda = 485$ nm, indicating a simple equilibrium (reaction 11). In contrast to that of $Co^{II}(salen)(py)_2$, the spectrum of $Co^{II}(salen)(DMF)(py)$ crosses the isopotential points. This proves that indeed *three* Co(II) species must be considered over the entire range of solvent compositions rather than two.

Construction and Analysis of Thermodynamic Cycles. Ladder Scheme 1 is composed of three thermodynamic cycles: One involves only the bis-DMF and the mixed solvated species {$Co^{II}(salen)(DMF)_2 \rightleftharpoons [Co^{III}(salen)(DMF)_2]^+ \rightleftharpoons [Co^{III}(salen)(DMF)(py)]^+ \rightleftharpoons Co^{II}(salen)(DMF)(py) \rightleftharpoons Co^{II}(salen)(DMF)_2$, cycle A; corresponding to the upper square scheme in Scheme 1, reaction 7}, one is composed of reactions between the mixed solvated and the bis-py complexes {$Co^{II}(salen)(DMF)(py) \rightleftharpoons [Co^{III}(salen)(DMF)(py)]^+ \rightleftharpoons [Co^{III}(salen)(py)_2]^+ \rightleftharpoons Co^{II}(salen)(py)_2 \rightleftharpoons Co^{II}(salen)(DMF)(py)$, cycle B; corresponding to the lower square scheme in Scheme 1}, and one involves all six complexes $[Co^{II}(salen)(DMF)_2 \rightleftharpoons [Co^{III}(salen)(DMF)_2]^+ \rightleftharpoons [Co^{III}(salen)(DMF)(py)]^+ \rightleftharpoons [Co^{III}(salen)(py)_2]^+ \rightleftharpoons Co^{II}(salen)(py)_2 \rightleftharpoons Co^{II}(salen)(DMF)(py) \rightleftharpoons Co^{II}(salen)(DMF)_2$; cycle C].

The three cycles are not independent, since C can be regarded as a combination of cycles A and B.

The four parameters characterizing cycle A (E^0_{DMF}, $K^{III}_{DMF/DMF,py}$, $E^0_{DMF/py}$, and $K^{II}_{DMF/DMF,py}$) have been determined in this work from independent experiments. From these values the consistency of the results can be checked. In particular, the validity of the assumptions leading to the determination of $E^0_{DMF/py}$ will be tested. As regards cycles B and C, one parameter, *viz.* $K^{III}_{py/DMF,py}$, could not be extracted from experimental data directly, since the voltammetric reduction peaks of $[Co^{III}(salen)(DMF)(py)]^+$ and $[Co^{III}(salen)(py)_2]^+$ were not sufficiently separated. If the other parameters in the ladder scheme were consistent, it would be possible to calculate this equilibrium constant from the K and E^0 known.

For the analysis of the thermodynamic cycles, both formal potentials and equilibrium constants were converted into Gibbs free energies according to

$$\Delta G^0 = -nFE^0 \tag{13}$$

(with $n = 1$) and

$$\Delta G^0 = -RT \ln K \tag{14}$$

($F = 96485$ C mol^{-1}, $R = 8.3144$J K^{-1}, $T = 298$ K). To prevent round-off errors, for the following analysis nonrounded values for ΔG^0 were used (Table 1).

Summation of all ΔG^0 over the reaction steps in cycle A yields $|\sum \Delta G^0| = 265(^{+1170}_{-1310})$ J mol^{-1}. The deviation from the expected value of zero is much smaller than the errors in the individual ΔG^0 and comprises only 0.5% of the total energy turnover $\sum|\Delta G°|$ in cycle A. We conclude that the thermodynamic parameters of the upper square scheme in Scheme 1 are consistent within their experimental uncertainty. In particular, the value of $E^0_{DMF/py}$ is consistent with the other results.

In both cycles B and C, we now use the relation $\sum \Delta G^0 = 0$ to calculate $K^{III}_{py/DMF,py}$. The results are again consistent and listed in Table 1.

Discussion

Coordination Geometry of Co^{II}(salen) Species. In accordance with our earlier, *qualitative* conclusions,[30] *quantitative* determination of the E^0 and K in the present work supports the notion of a three-rung ladder scheme for solvent exchange in the system **1**/**1**$^+$. All results are readily explained in the context of Scheme 1, which requires hexacoordination for both the Co(III) and the Co(II) species.

While the formulation of the Co(III) complexes in Scheme 1 as hexacoordinated 18-electron species is straightforward, the question of the coordination number and geometry of Co^{II}(salen) species is controversial in the literature. Often, pentacoordinated Co^{II}(salen)-type complexes are formulated, which reflects results of X-ray analyses[66,67] and ESR spectroscopy,[18,24] the latter in solutions with only a *small amount of base* present (toluene + 1% py). On the other hand, Co(II) was characterized in *neat* DMF solution as being coordinated by six DMF molecules,[68] and complexes structurally similar to **1** have been formulated in hexacoordinate form.[20] Recently, equilibria between penta- and hexacoordinated macrocyclic complexes of Co(II) have been invoked to explain electrochemical results.[69]

The UV/vis data presented here show clearly that indeed three distinct Co(II) complexes must be present in the DMF/py solvent system, and according to the ladder scheme, these must be hexacoordinated. Additional equilibria to form pentacoordinated complexes cannot be excluded on the basis of the data reported. None of the experimental data, however, requires assumption of dissociation to pentacoordinate species.[70]

On the other hand, the results do not provide information about the type of bonding between the solvent molecules and the Co central atom, nor do they suggest that the bonds to the two axially coordinated ligands are equal. In the case of Co(II), one of the axially bound molecules could well belong to the "solvation shell" of the complex. The data do, however, show that there is a measurable interaction of the Co central atom with two axial ligands.

Thermodynamic Parameters in Ladder Scheme 1. In the three-rung ladder Scheme 1 seven reactions are coupled which entails the major problem in an attempt to determine the formal potentials and equilibrium constants. In the present case, however, the positions of the equilibria can be shifted by changes of the solvent composition. By proper choices of the experimental conditions the ladder scheme was reduced to several more simple reaction sequences: quasi-reversible electron transfers (eqs 1 and 2), the CE mechanism (eq 3), an equilibrium between two electroactive species which is frozen in the experimental time scale (in eq 7), the $E_{qr}\underline{C}$ mechanism (eq 10), and finally exchange equilibria (e.g., eq 11).

The *redox potential* of the cobalt Schiff-base complexes shifts to considerably more negative values if a stronger electron pair donor (py) is replacing a weaker one (DMF) in the axial positions. This is in accordance with earlier reports[26,29] where E^0 had been determined in plain solvents and correlated with the donor number. No exchange reactions were, however, described in these investigations. Carter et al.[24] found only small shifts of E^0 for cobalt acetylacetoniminato or TPP complexes when the solvent was changed from py to 4% py−CH_3CN or to 4% py−DMF. Probably, under their conditions, both solvents (i.e., donor molecules) were present in a large excess relative to the complex, not revealing the exchange reactions. The variation of the solvent exchange equilibrium (corresponding to $K^{II}_{py/DMF,py}$) may have been too small to cause measurable shifts of $\bar{E}$ (flat part on left side of the $\bar{E}$ vs x_{DMF} curve in Figure 2b). According to the results of the present work the solvent effect on E^0 must be attributed to the *exchange* of *two* axial donor molecules.

From the *equilibrium constants* it is evident that the stronger donor predominantly binds to the Co atom in three of the four equilibria in Scheme 1. Only the second exchange reaction in the Co(II) state is slightly in favor of bonding the weaker donor. In the Co(salen) type complexes the quadridentate Schiff-base ligand is arranged almost planar,[36,48,66] forming a 14- or 15-electron complex fragment without the axial ligands. A maximum of two solvent ligands may interact in axial direction, leading to an 18-electron complex for Co(III) and to a 19-electron complex for Co(II) systems.

$[Co(salen)]^+$ is a stronger Lewis acid than the neutral Co(salen). It prefers to interact with py which is a stronger donor than DMF, characterized by large equilibrium constants $K^{III}_{DMF/DMF,py}$ and $K^{III}_{py/DMF,py}$. On the other hand, the electron

(66) Brückner, S.; Calligaris, M.; Nardin, G.; Randaccio, L. *Acta Crystallogr.* **1969**, *B25*, 1671−1674.
(67) Bresciani, N.; Calligaris, M.; Nardin, G.; Randaccio, L. *J. Chem. Soc., Dalton Trans.* **1974**, 498−502.
(68) Yokoyama, H.; Suzuki, S.; Goto, M.; Shinozaki, K.; Abe, Y.; Ishiguro, S. *Z. Naturforsch.* **1995**, *50a*, 301−306.
(69) Kang, C.; Anson, F. C. *J. Electroanal. Chem.* **1996**, *407*, 233−236.

(70) Additional electrochemical experiments prove indeed that the assumption of two pentacoordinate complexes Co^{II}(salen)(L^1) and Co^{II}(salen)(L^2) cannot explain the shift of $\bar{E}$ in mixtures of two donor solvents. The results allow the estimation of equilibrium constants for the formation of such species from the hexacoordinated forms and show that the hexacoordinate complexes are predominant in various systems L^1/L^2: Eichhorn, E.; Rieker, A.; Speiser, B., manuscript in preparation.

excess in the Co(II) complexes will be meliorated by ligation of a weaker donor (here DMF). Consequently, bonding of py is less preferred and even disadvantageous in the case of $K^{II}_{py/DMF,py}$. Still, however, a large excess of py forces formation of $Co^{II}(salen)(py)_2$.

The main solvent effect on $E^0(\mathbf{1}/\mathbf{1}^+)$ when exchanging DMF vs py (40 kJ mol^{-1}) can be explained by the thermodynamics of the exchange equilibria in the Co(III) oxidation state. While the substitution of two DMF ligands by two py molecules in the Co(II) complex yields only a change of $\Delta G^0 \approx 9.5$ kJ mol^{-1}, the analogous reaction stabilizes the Co(III) species by about 49 kJ mol^{-1}. Consequently, we interpret the effect of the "donor number" of the solvent on $E^0(\mathbf{1}/\mathbf{1}^+)$ as a strongly increased stabilization of the Co(III) complexes by the stronger donor: E^0 decreases due to the increased stability of the bis-py complex in the oxidized Co(III) form.

As frequently observed, the equilibrium constants for the second exchange reactions in either oxidation state are smaller than those for the first ones. For the Co(III) complexes $K^{III}_{py/DMF,py}/K^{III}_{DMF/DMF,py} \approx 0.3$ is very close to the value of 0.25 predicted for statistical exchange equilibria.[71] No particular sterical or electronic interaction seems to be present. On the other hand, $K^{II}_{py/DMF,py}/K^{II}_{DMF/DMF,py} \approx 0.015$ is much smaller than the statistical value. This indicates a change of the bonding to the axial ligands. A py ligand may possibly act as a π-back-bonding ligand,[72] thus decreasing electron density at Co(II). A simple donor base such as DMF is not able to exert such an interaction. Bonding of the first py becomes more favorable, and this decreases the ratio of equilibrium constants.

Cross Reaction Equilibria. Although the seven ET and solvent exchange reactions discussed so far fully describe the thermodynamics of ladder Scheme 1, additional equilibria can be formulated. As in a simple square scheme,[31] these are cross reactions, in the present example reactions 15−17. Equilibrium

$$[Co^{III}(salen)(DMF)_2]^+ + Co^{II}(salen)(DMF)(py) \rightleftharpoons Co^{II}(salen)(DMF)_2 + [Co^{III}(salen)(DMF)(py)]^+ \quad (15)$$

$$[Co^{III}(salen)(DMF)(py)]^+ + Co^{II}(salen)(py)_2 \rightleftharpoons Co^{II}(salen)(DMF)(py) + [Co^{III}(salen)(py)_2]^+ \quad (16)$$

$$[Co^{III}(salen)(DMF)_2]^+ + Co^{II}(salen)(py)_2 \rightleftharpoons Co^{II}(salen)(DMF)_2 + [Co^{III}(salen)(py)_2]^+ \quad (17)$$

17 corresponds to the sum of reactions 15 and 16, which again shows the intimate mutual dependence of the three thermodynamic cycles in Scheme 1. Each cross reaction corresponds to an electron transfer between two complex species or to a combination of solvent exchanges. Several further "complex interaction equilibria" may be considered, but all of them are combinations of reactions 15 and 16 and/or of simple solvent exchanges. The equilibrium constants for each of these processes can be derived from the data in Table 1, and $K = 690^{+330}_{-200}$ is found for reaction 15 and $K = (1.3^{+1.1}_{-0.55}) \times 10^3$ for reaction 16. Although no additional thermodynamic information is gained, the complex interactions may affect the kinetics within ladder Scheme 1.

All analyses presented in this paper, except the determination of $E^0_{DMF/py}$, were based on data measured under equilibrium conditions. The value of $E^0_{DMF/py}$ could have been influenced by cross reaction kinetics. It fits, however, very well into the other results for the equilibria in cycle A. This shows that complications due to the complex interaction equilibria are not important in the present case and under the conditions used.

(71) In ref 81, p 44.
(72) Further experiments to elucidate this effect in the present systems are currently under way.

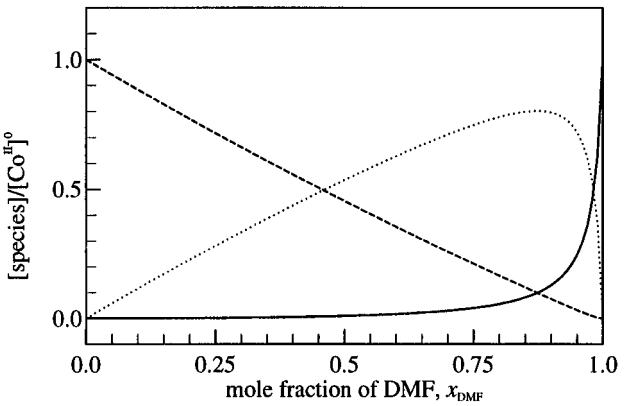

Figure 5. Distribution of Co(II) species for **1** in DMF/py mixtures, concentrations of species normalized to total complex concentration: $Co^{II}(salen)(DMF)_2$ (solid line), $Co^{II}(salen)(DMF)(py)$ (dotted line), $Co^{II}(salen)(py)_2$ (broken line).

Distribution of Co^{II}(salen) and Co^{III}(salen) Species in DMF/py Mixtures. The data reported in the present paper allow one to estimate the distribution of the variously substituted Co(II) or Co(III) species in a solvent mixture of DMF and py with a given composition, provided the total complex concentration is known.

Equations to determine [species]/$[Co^{II/III}]^0$([species] is the concentration of a particular species) are given in the Supporting Information. In both the Co(II) and the Co(III) oxidation state the fraction of the bis-DMF complex monotonously decreases with decreasing x_{DMF}, while the fraction of the bis-py complex increases and that of the mixed complex passes through a maximum (species distribution diagrams in Figures 5 and 6).

Owing to the small values of the equilibrium constants $K^{II}_{DMF/DMF,py}$ and $K^{II}_{py/DMF,py}$, appreciable concentrations of py-containing Co(II) complexes are only observed if $[py]^0$ is considerably larger than the total complex concentration used. This is true for all $[Co^{II}]^0$ up to the saturation concentration of **1** in DMF. Thus, for all practical purposes, the actual concentration of free py, [py], can be regarded as equal to $[py]^0$, and the species distribution diagram in Figure 5 is independent of $[Co^{II}]^0$.

On the other hand, $K^{III}_{DMF/DMF,py}$ and $K^{III}_{py/DMF,py}$ are large and even for $[py]^0 < [Co^{III}]^0$ measurable concentrations of py-substituted Co(III) complexes are present. Consequently, the equilibrium concentration [py] deviates from $[py]^0$. If we calculate x_{DMF} from the solvent composition in equilibrium, the diagram in Figure 6a is valid for all $[Co^{III}]^0$. Since the equilibrium values of [py] and [DMF] are not easily accessible experimentally, while $[py]^0$ and $[DMF]^0$ are always known, it is of more practical value to define the species distribution on the basis of the initial mole fraction of DMF, $x^0_{DMF} = [DMF]^0/([py]^0 + [DMF]^0)$. Such curves are given in Figure 6b−d, where the mole fraction axis has been recalculated taking into account the loss of py by complexation. Now, the distribution curves depend on $[Co^{III}]^0$, and curves for several values of the total complex concentration are given.

The diagrams in Figures 5 and 6 clearly show the problems we encountered when we tried to separate signals for the mixed solvated complexes. In the Co(II) series, for example, at the solvent composition where $[Co^{II}(salen)(DMF)(py)]/[Co^{II}]^0$ reaches a maximum (≈0.8), both other complexes are still present in a relative concentration of about 10%. In the Co(III) oxidation state the situation is even worse with $[[Co^{III}(salen)(DMF)(py)]^+]/[Co^{III}]^0$ only about 0.5 at the maximum. It is thus impossible

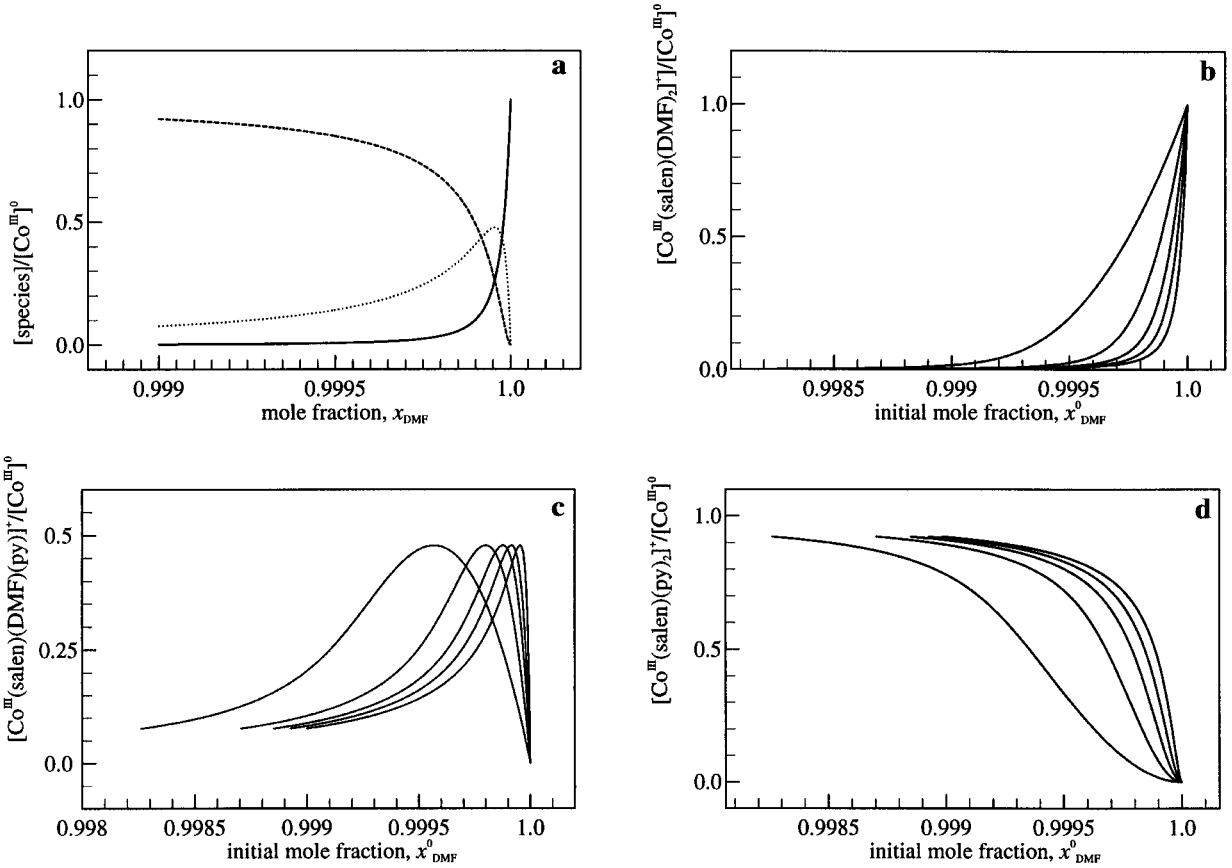

Figure 6. Distribution of Co(III) species for $\mathbf{1}^+$ in DMF/py mixtures, concentrations of species normalized to total complex concentration: (a) x_{DMF} calculated from solvent composition in equilibrium, $Co^{II}(salen)(DMF)_2$ (solid line), $Co^{II}(salen)(DMF)(py)$ (dotted line), $Co^{II}(salen)(py)_2$ (broken line); (b−d) x^0_{DMF} recalculated from x_{DMF}, curves for infinite dilution of the complex ($[Co^{III}]^0 \rightarrow 0.0$ mM), and $[Co^{III}]^0 = 0.5$, 1.0, 2.0, and 5.0 mM, with increasing $[Co^{III}]^0$ curves shift left, (b) $[Co^{III}(salen)(DMF)_2]^+$, (c) $[Co^{III}(salen)(DMF)(py)]^+$, and (d) $[Co^{III}(salen)(py)_2]^+$.

to find solvent conditions where the presence of the bis-DMF and the bis-py complexes can be neglected as compared to the mixed complex for both oxidation states of the central atom.

From Figure 5 the assumption used in the analysis of the UV/vis spectra can be demonstrated: For $x_{DMF} > 0.9$ the concentration of $Co^{II}(salen)(py)_2$ can be neglected. Similarly, for the Co(III) complexes it can be deduced that at $x_{DMF} < 0.95$ $[Co^{III}(salen)(py)_2]^+$ is dominant, and the Co(III) equilibria are indeed shifted strongly to the bis-py form (Figure 6).

Mechanistic Consequences for the Application of Co(salen) in Oxygenation Reactions. There are two results from our investigations which are crucial for the understanding of at least partial aspects of the complex Co(Schiff base)-catalyzed oxygenations of organic substrates.

As a first consequence of the interaction of **1** and $\mathbf{1}^+$ with the axial ligands, a change of the solvent composition affects any electron transfer involved in catalytic oxygenations with **1** through the redox potential. Upon complexation with a stronger donor molecule the Co(II) complexes are converted into stronger reducing agents, while the Co(III) complexes become weaker oxidants. The resulting potential shift (>400 mV in going from DMF to py) is much larger than the effect of substitution in the aromatic rings of the salen ligand [only 95 mV in going from Co(dinitro-salen) to Co(dimethoxy-salen)].[73]

In particular, the continuous change of $\bar{E}$ with the solvent composition provides a way to tune the redox properties of the Co(salen) catalyst in a wide range of potentials, which may be important for the use of **1** or $\mathbf{1}^+$ as mediators or as redox agents. The oxidative addition of *o*-quinones to Co(Schiff base) complexes, for example, is controlled by the redox potential of the complex and thus depends on the solvent.[74]

The binding ability of O_2 to Co(salen)-type complexes depends on the basicity of the axial ligands[4] and is related to their redox potential.[22,24,75] Consequently, changes in axial ligands will modulate the thermodynamics of O_2 activation. Furthermore, axial substituents have been found to accelerate oxygenations by salen-analogue complexes with increasing donor strength.[76] Hence, a change of solvation of the cobalt center also changes the kinetics of the oxygen transfer reaction.

As a second consequence, the exchange of DMF vs py in **1** or $\mathbf{1}^+$ may be regarded as a model for the interaction of the Co complexes with substrates during the oxygenation reaction. If indeed the substrate is activated by complexation, it has to be basic enough in order to substitute a solvent molecule, which is usually present in large excess, in the solvated complex. On the other hand, if binding of the substrate or the product to the complex is too strong, the catalyst may become inactive. Similar arguments hold for the oxidant itself, which must be coordinated to the central atom, at least for an "inner-sphere oxygenation" process. Indeed, oxygen activation by **1** probably requires substitution of a solvent by an O_2 molecule,[19,20] and again the solvent exchange is a model for this reaction step.

Thus, complete knowledge of ladder schemes involving solvent, substrate, and oxygen source as axial ligands would be necessary to describe each oxygenation experiment. How-

(73) Nishinaga, A.; Tajima, K.; Speiser, B.; Eichhorn, E.; Rieker, A.; Ohya-Nishiguchi, H.; Ishizu, K. *Chem. Lett.* **1991**, 1403−1406.

(74) Hartl, F.; Vlček, A., Jr. *Inorg. Chim. Acta* **1986**, *118*, 57−63.

(75) Puxeddu, A.; Costa, G. *J. Chem. Soc., Dalton Trans.* **1981**, 1115−1119.

(76) Böttcher, A.; Elias, H.; Jäger, E.-G.; Langfelderova, H.; Mazur, M.; Müller, L.; Paulus, H.; Pelikan, P.; Rudolph, M.; Valko, M. *Inorg. Chem.* **1993**, *32*, 4131−4138.

Scheme 2. Oxygenation of 3-Hydroxyflavones with Co(salen)[5] (top) and Activation of Co(salen)−Flavonole Complex in DMF (Bottom)

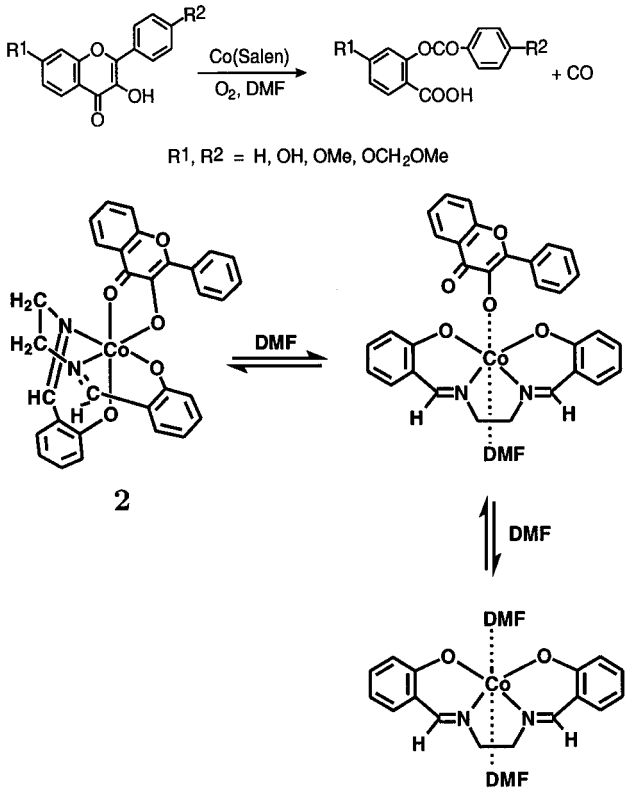

ever, some peculiarities mentioned in the Introduction can already be explained with the results of the present investigation.

The solvent effect on the oxygenation of phenolic flavonols[5] (Scheme 2) is one example. For the oxygenation of phenols the formation of a $Co^{III}(salen)^+(phenolate)^-(S)$ complex (S = solvent) seems to be essential. This may be attained *via* deprotonation of the phenol by the primary peroxyl complex $Co^{III}(salen)^+O_2^{\bullet-}$ or $Co^{III}(salen)$ OH produced from $Co^{II}(salen)$ and O_2.[77] The $Co^{III}(salen)^+(phenolate^-)(S)$ complex further reacts with oxygen to yield the oxygenation products.[78] Analogously, flavonol would first give the flavonolate.

Qualitative results have already shown that in DCM solutions similar ladder schemes are operative.[30] In the weakly donating solvent DCM the flavonolate is able to replace both DCM molecules in $[Co^{III}(salen)(DCM)_2]^+$, one by its phenolate-oxygen, the other one by the keto-oxygen. The resulting $Co^{III}(salen)^+(\eta^2$-flavonolate$^-)$ (**2**) is completely inert toward O_2 and can even be isolated. Its crystal structure was determined, showing a strongly distorted salen framework.[23] If this complex is dissolved in DMF, oxygenation starts immediately. Obviously, the stronger basic DMF oxygen[79] detaches the flavonol keto-oxygen from the Co atom to give a new complex $Co^{III}(salen)^+(\eta^1$-flavonolate$^-)$(DMF) with the usual salen geometry, in which flavonolate acts as a monodentate ligand. As a normal phenolate complex, it is susceptible to O_2 insertion as such or the phenolate itself reacts with O_2 after displacement by a second DMF molecule.[21]

Another example is the oxygenation of indole to *N*-formylaminoacetophenone with $Co^{II}(salen)/O_2$:[8] In DCM the reaction proceeds faster than in DMF. Again the substrate indole must first replace a solvent molecule S from $[Co^{III}(salen)(S_2)]^+$. This can easily be done for S = DCM but is much more difficult for S = DMF. The formamide derivative formed in the reaction can be displaced from the coordination sphere by the more basic indole. Addition of the even stronger base *N*-methylimidazole suppresses the reaction completely;[8] for pyridine the same effect is expected. Such basic molecules coordinate to the central atom instead of the less basic substrate and in this way block the catalyst.

As a consequence, the oxygenation reaction generally can only proceed well if the substrate is more basic than the solvent and the educt is more basic than the product.

Conclusion

Variation of the solvent composition made it possible to thermodynamically characterize all individual ET and ligand exchange reactions in ladder Scheme 1 for the interaction of **1** and $\mathbf{1}^+$ with DMF and py.

The results are important for the understanding of catalyst−substrate interactions which seem to be crucial for the oxygenation process, at least, if an inner-sphere mechanism holds. Similar experiments will have to be performed with substrate molecules and oxygen as ligands, before the combined and concerted action of substrate and oxygen on the catalyst, which represents the more complex reality of oxygenation, can be disclosed. Such experiments are currently in progress.

Acknowledgment. The authors thank the Volkswagen-Stiftung, Hannover, Germany, and the Fonds der Chemischen Industrie, Frankfurt/Main, Germany, for financial support of this work. B.S. thanks the Deutsche Forschungsgemeinschaft, Bonn, Germany, for a Heisenberg fellowship. E.E. was supported by the Land Baden-Württemberg (doctoral fellowship).

Supporting Information Available: Tables of voltammetric data and results for equilibrium constants and formal potentials from individual experiments and equations for the calculation of species distribution diagrams (7 pages). Ordering information is given on any current masthead page.

IC9703336

(77) Nishinaga, A.; Shimizu, T.; Toyoda, Y.; Matsuura, T.; Hirotsu, K. *J. Org. Chem.* **1982**, *47*, 2278−2285.
(78) Yoshioka, Y.; Yamanaka, S.; Yamada, S.; Kawakami, T.; Nishino, M.; Yamaguchi, K.; Nishinaga, A. *Bull. Chem. Soc. Jpn.* **1996**, *69*, 2701−2722.
(79) X-ray analysis of $Co^{III}(salen)(DMF)_2^+PF_6^-$ shows that DMF is coordinated via the oxygen atom; see ref 36.
(80) Bard, A. J.; Faulkner, L. R. *Electrochemical Methods. Fundamentals and Applications*; John Wiley: New York, 1980.
(81) Cotton, F. A.; Wilkinson, G. *Advanced Inorganic Chemistry*; Wiley: New York, 1988.